Supporting Information for

Fine-Tuning Terminal Solvent Ligands to Rationally Enhance the Energy Barrier in Dinuclear Dysprosium Single-Molecule Magnets

Kun Zhang,[a] Chen Yuan,[b] Fu-Sheng Guo,[a] Yi-Quan Zhang*[b] and Yao-Yu Wang*[a]

[a] Shaanxi Key Laboratory of Physico-Inorganic Chemistry, Key Laboratory of Synthetic and Natural Functional Molecule Chemistry of the Ministry of Education, College of Chemistry & Materials Science, Northwest University, Xi'an, 710069, P.R.China

[b] Jiangsu Key Laboratory for NSLSCS, School of Physical Science and Technology, Nanjing Normal University, Nanjing 210023, P. R.China.

e-mail: wyaoyu@nwu.edu.cn; zhangyiquan@njnu.edu.cn.

Supplementary Information Contents

Table S1 Crystallographic data for complexes **1** and **2**.

Complex	**1**	**2**
Formula	$C_{66}H_{60}Dy_2N_6O_{14}$	$C_{76}H_{82}Dy_2N_8O_{16}$
Fw	1486.20	1688.49
Temp (K)	296(2)	100(2)
Crystal system	Monoclinic	Monoclinic
Space group	*C2/c*	$P2_1/n$
a (Å)	26.984(16)	17.6437(7)
b (Å)	10.811(7)	12.2553(5)
c (Å)	21.325(13)	18.4911(8)
α (°)	90.00	90.00
β (°)	103.361(11)	113.017(1)
γ (°)	90.00	90.00
Volume (Å^3)	6053(6)	3680.0(3)
Z	4	2
D_{calc} (g cm^{-3})	1.631	1.524
μ (mm^{-1})	2.522	2.087
F (000)	2968	1708
Reflections (all)	4918	9032
Reflections(> 2σ)	3566	6872
R_{int}	0.0583	0.0658
R_{sigma}	0.0682	0.0401
R_1, wR_2 ($I > 2\sigma(I)$)	0.0444, 0.1142	0.0824, 0.1869
R_1, wR_2 (all data)	0.0686, 0.1277	0.1118, 0.2055
GOF	0.996	1.050

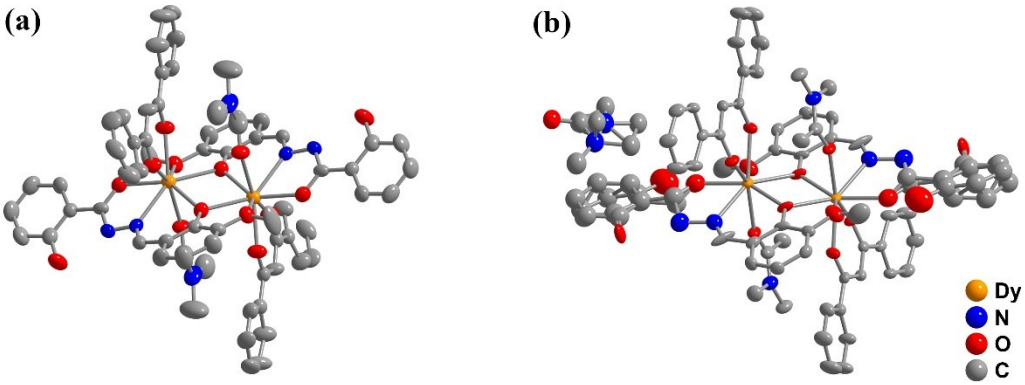

The ORTEP-style plots for complexes **1** (a) and **2** (b).

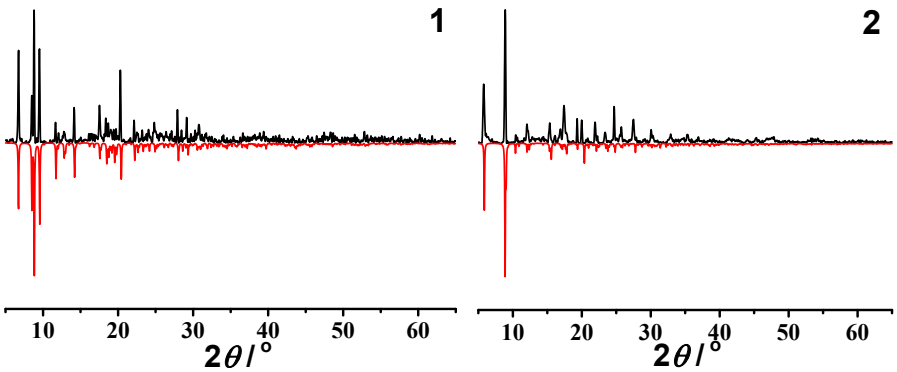

Figure S1. The experimental (black) powder X-ray diffraction and simulated patterns (red) of **1** and **2**.

Table S2 Selected bond lengths (Å) and angles (°) for complexes **1** and **2**

	1	**2**
Dy1-O1	2.316(5)	2.317(6)
Dy1-O1[a]	2.337(5)	2.361(6)
Dy1-O2	2.252(5)	2.289(10)
Dy1-O3[a]	2.487(5)	2.636(9)
Dy1-O5	2.407(5)	2.296(7)
Dy1-O6	2.244(5)	2.290(6)
Dy1-O7	2.278(5)	2.355(6)
Dy1-N1	2.436(7)	2.437(10)
Dy1-O1-Dy1[a]	106.5(2)	105.3(2)
O1-Dy1-O1[a]	73.5 (2)	74.7(2)

Symmetry transformations used to generate equivalent atoms : for **1**, a: 2-x, -y, 2-z; for **2**, a: 1-x, 1-y, 1-z.

Table S3. SHAPE analysis of the Dy(III) ion in complexes **1** and **2**

Label	Shape	Symmetry	Distortion (**1**)	Distortion (**2**)
OP-8	Octagon	D_{8h}	27.165	26.537
HPY-8	Heptagonal pyramid	C_{7v}	26.026	19.021
HBPY-8	Hexagonal bipyramid	D_{6h}	26.126	17.262
CU-8	Cube	O_h	27.305	16.880
SAPR-8	Square antiprism	D_{4d}	17.868	8.307
TDD-8	Triangular dodecahedron	D_{2d}	15.836	7.329
JGBF-8	Johnson gyrobifastigium J26	D_{2d}	20.983	14.508
JETBPY-8	Johnson elongated triangular bipyramid J14	D_{3h}	21.365	22.954
JBTPR-8	Biaugmented trigonal prism J50	C_{2v}	11.029	4.215
BTPR-8	Biaugmented trigonal prism	C_{2v}	14.527	5.825
JSD-8	Snub diphenoid J84	D_{2d}	11.590	5.690
TT-8	Triakis tetrahedron	T_d	26.846	16.867
ETBPY-8	Elongated trigonal bipyramid	D_{3h}	26.183	23.268

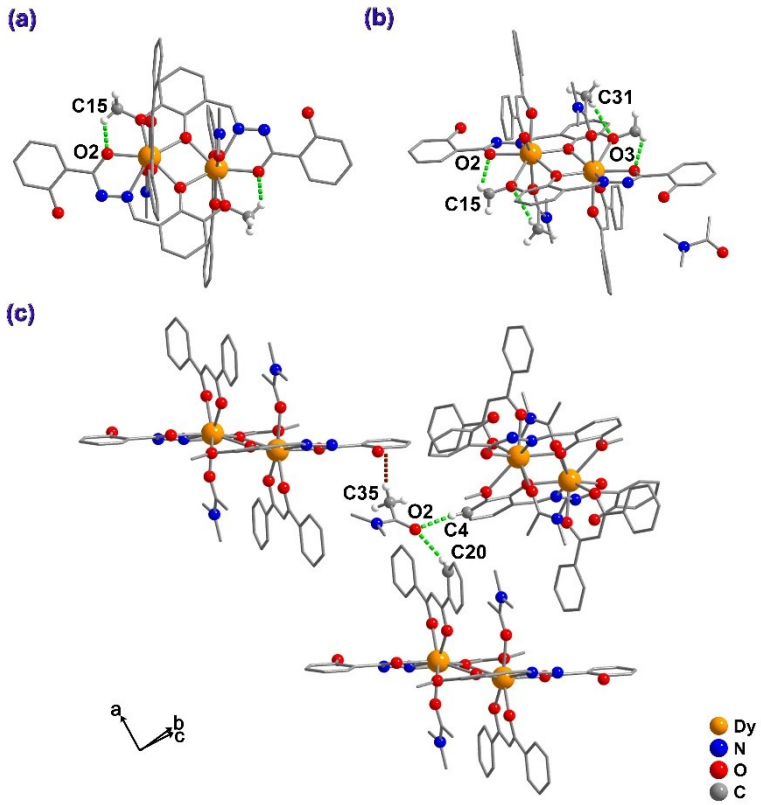

Figure S2. The intramolecular hydrogen bond (green dashed line) of **1** (a) and the intra (b) and inter (c) molecular hydrogen bond (green dashed line) and C-H··· π interaction (brown dashed line) of **2**.

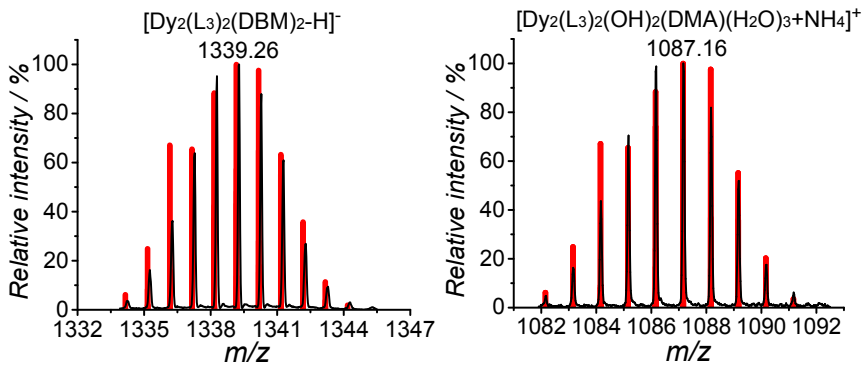

Figure S3. Red bars correspond to the simulated mass spectrometry data and black lines correspond to the experimental mass spectrometry data for complexes **1** (left) and **2** (right). All calculated peaks fit the statistical treatment of experimental error.

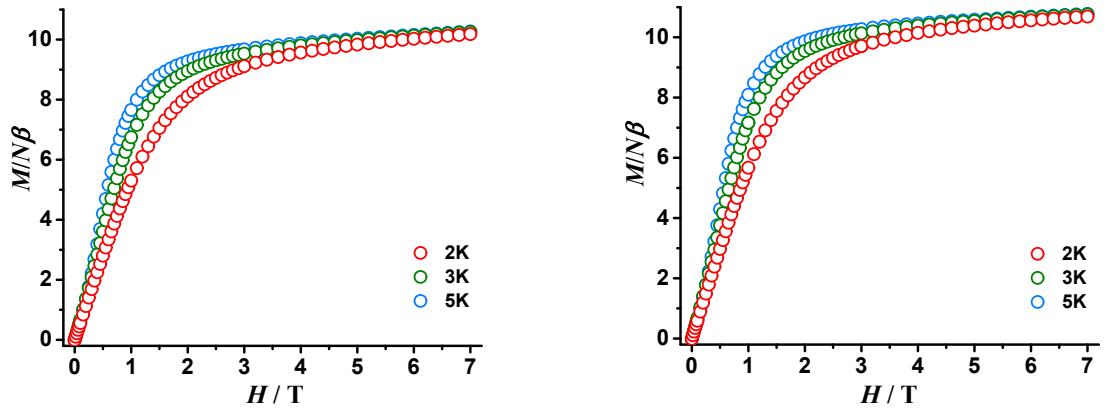

Figure S4. Field dependence of the magnetization, M, at 2, 3 and 5 K for for complexes **1** and **2** plotted as *M vs. H.*

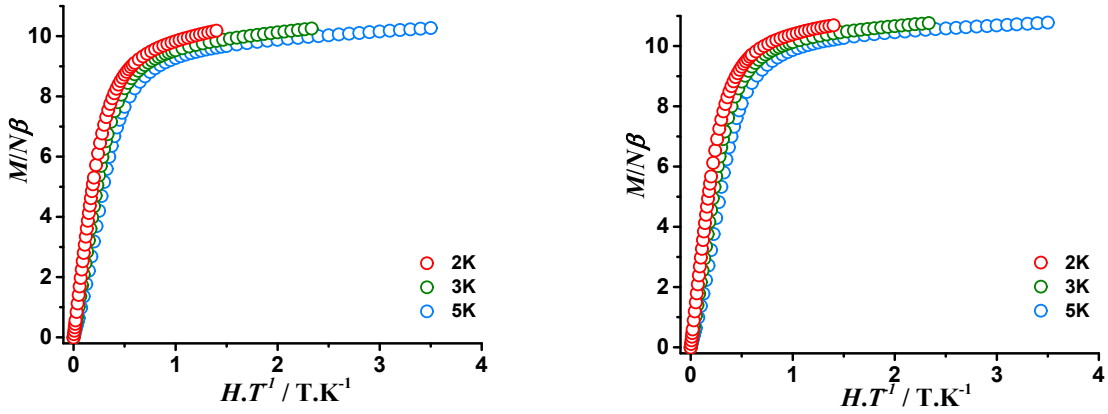

Figure S5. Field dependence of the magnetization, M, at 2, 3 and 5 K for for complexes **1** and **2** plotted as *M vs. H* T^{-1}.

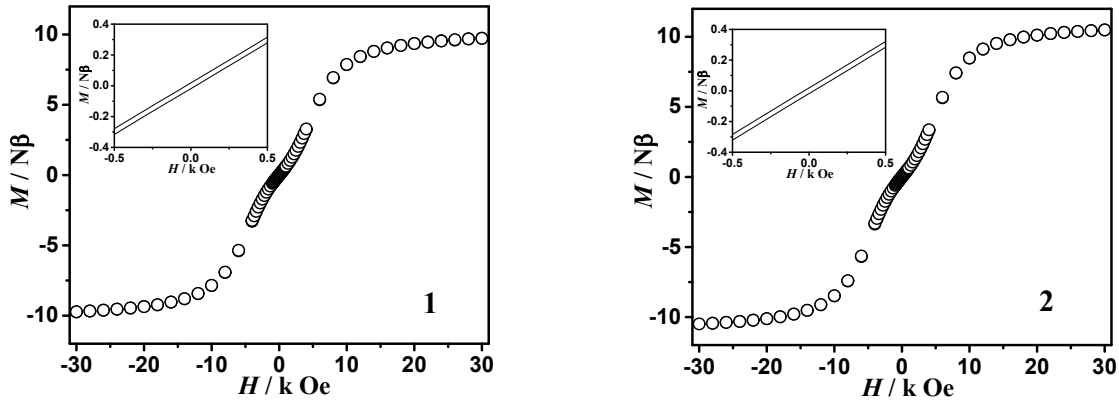

Figure S6. Magnetic hysteresis loops at 1.8 K for complexes **1** and **2**.

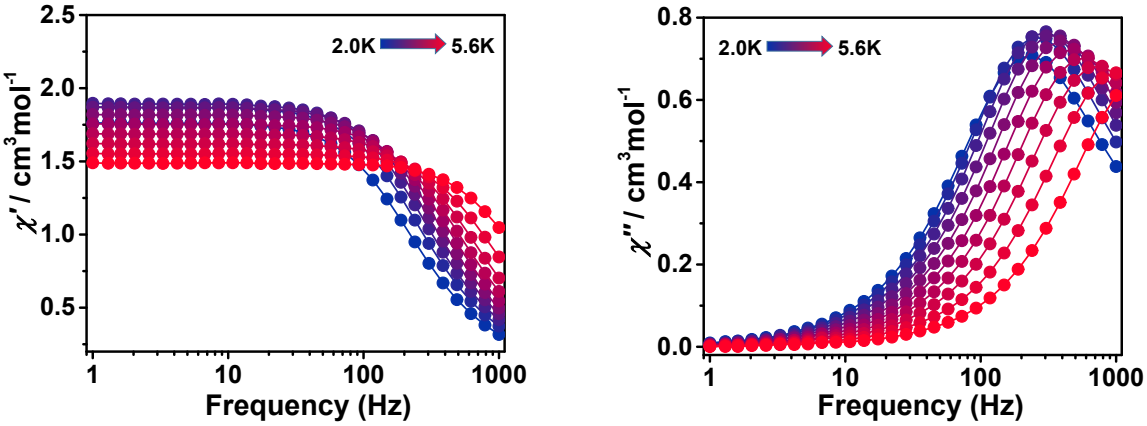

Figure S7a. Frequency dependence in zero dc field of the in-phase (χ', left) and the out-of-phase (χ'', right) ac susceptibility component at different temperature for **1**.

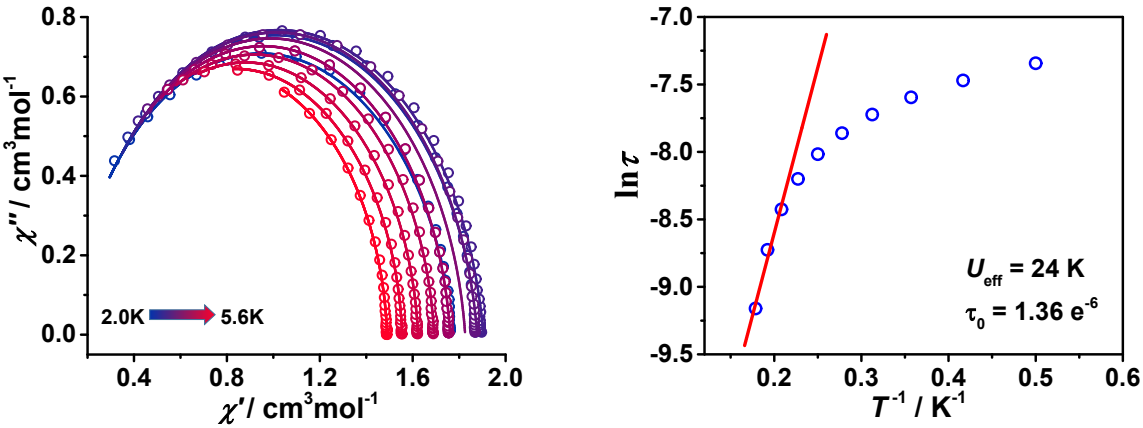

Figure S7b. Cole-Cole plot (left) using the ac susceptibility data shown in Figure S7a for **1**. The solid lines are the best fit obtained with a generalized Debye model. Plot of ln(τ), where τ is the relaxation time of the magnetization, vs 1/T for **1** (right). The red line represent the best fit to the Arrhenius law of the thermally activated region. The effective energy barriers (U_{eff}) obtained from the fits are indicated.

Table S4. Relaxation fitting parameters from Least-Squares Fitting of χ(*f*) between 1-997 Hz data under zero dc field of complex **1**

Temperature	χ_T	χ_s	α	τ
2.0K	1.77	0.12	0.10	6.47E-4
2.4K	1.88	0.13	0.09	5.69E-4
2.8K	1.90	0.15	0.09	5.03E-4
3.2K	1.88	0.15	0.08	4.42E-4
3.6K	1.82	0.15	0.07	3.85E-4
4.0K	1.76	0.15	0.06	3.30E-4
4.4K	1.69	0.14	0.06	2.75E-4
4.8K	1.62	0.14	0.05	2.19E-4
5.2K	1.55	0.12	0.04	1.62E-4
5.6K	1.49	0.07	0.04	1.05E-4

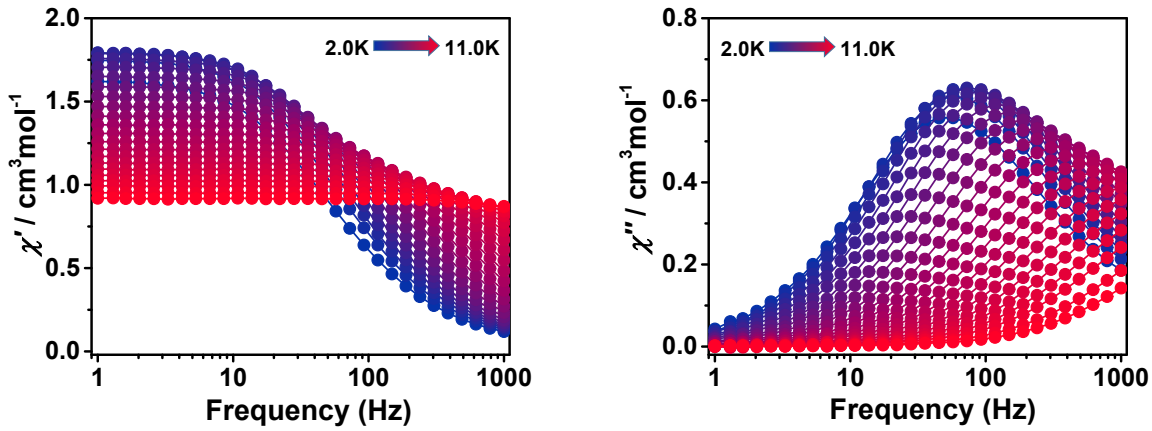

Figure S8a. Frequency dependence in zero dc field of the in-phase (χ', left) and the out-of-phase (χ'', right) ac susceptibility component at different temperature for **2**.

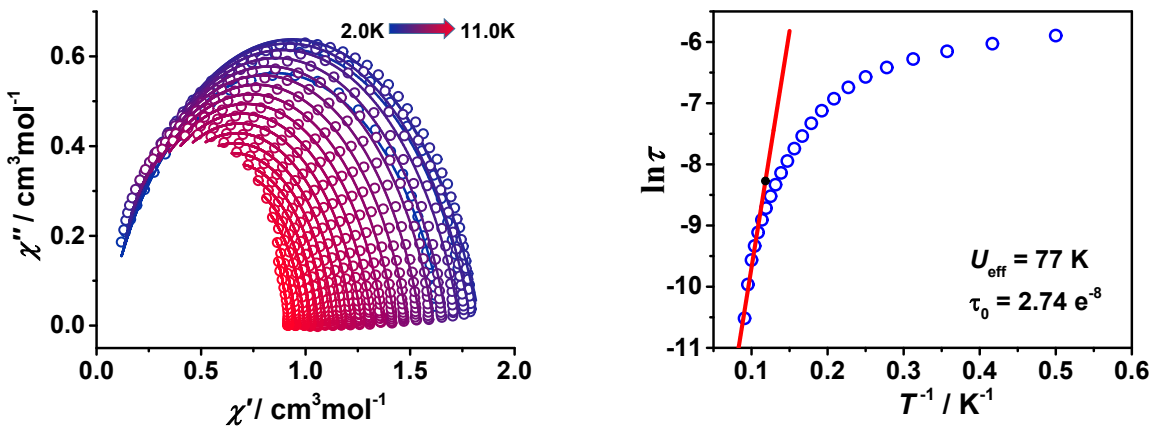

Figure S8b. Cole-Cole plot (left) using the ac susceptibility data shown in Figure S8a for **2**. The solid lines are the best fit obtained with a generalized Debye model. Plot of ln(τ), where τ is the relaxation time of the magnetization, vs 1/T for **2** (right). The red line represent the best fit to the Arrhenius law of the thermally activated region. The effective energy barriers (U_{eff}) obtained from the fits are indicated.

Table S5. Relaxation fitting parameters from Least-Squares Fitting of $\chi(f)$ between 1-997 Hz data under zero dc field of complex **2**

Temperature	χ_T	χ_s	α	τ
2.0K	1.67	0.04	0.23	0.003
2.4K	1.79	0.06	0.22	0.002
2.8K	1.84	0.04	0.21	0.002
3.2K	1.83	0.04	0.21	0.002
3.6K	1.79	0.04	0.21	0.002
4.0K	1.74	0.04	0.20	0.001
4.4K	1.68	0.04	0.20	0.001
4.8K	1.61	0.04	0.19	9.81E-4
5.2K	1.55	0.04	0.19	8.05E-4
5.6K	1.49	0.04	0.19	6.56E-4
6.0K	1.43	0.05	0.18	5.32E-4
6.4K	1.37	0.06	0.18	4.33E-4
6.8K	1.32	0.07	0.17	3.54E-4
7.2K	1.27	0.10	0.16	2.91E-4
7.6K	1.22	0.12	0.16	2.40E-4
8.0K	1.18	0.15	0.15	1.99E-4
8.4K	1.14	0.17	0.14	1.64E-4
8.8K	1.10	0.21	0.13	1.35E-4
9.2K	1.06	0.23	0.12	1.10E-4
9.6K	1.03	0.25	0.12	8.83E-5
10.0K	0.99	0.26	0.11	7.02E-5
10.5K	0.95	0.25	0.10	4.70E-5
11.0K	0.92	0.10	0.10	2.71E-5

Computational details

Complete-active-space self-consistent field (CASSCF) calculations on the Dy fragments (see Figure S9 for the model structure of complexes **1** and **2**) of complexes **1** and **2** on the basis of X-ray determined geometry have been carried out with MOLCAS 8.0 program package.[S1] For CASSCF calculations, the basis sets for all atoms are atomic natural orbitals from the MOLCAS ANO-RCC library: ANO-RCC-VTZP for Dy(III) ion; VTZ for close O and N; VDZ for distant atoms. The calculations employed the second order Douglas-Kroll-Hess Hamiltonian, where scalar relativistic contractions were taken into account in the basis set and the spin-orbit coupling was handled separately in the restricted active space state interaction (RASSI-SO) procedure. The active electrons in 7 active spaces include all f electrons CAS (9 in 7) for complexes **1** and **2** in the CASSCF calculation. To exclude all the doubts we calculated all the roots in the active space. We have mixed the maximum number of spin-free state which was possible with our hardware (all from 21 sextets, 128 from 224 quadruplets and 130 from 490 doublets for Dy(III) fragments).

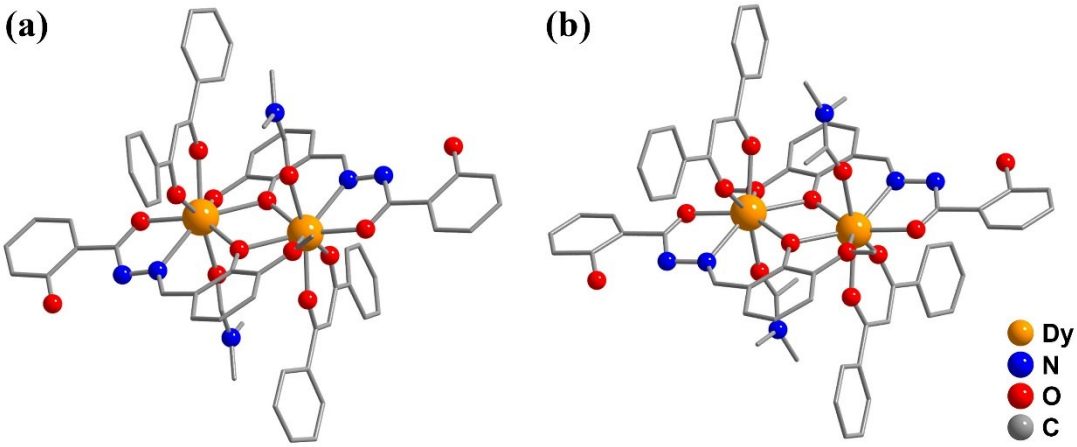

Figure S9. Calculated Dy fragment of complexes **1** (a) and **2** (b); Hydrogen atoms and solvent molecules have been omitted.

To fit the exchange interactions in complexes **1** and **2**, we took two steps to obtain them. Firstly, we calculated one Dy(III) fragment using CASSCF to obtain the corresponding magnetic properties. Then, the exchange interaction between the magnetic centers is considered within the Lines model,[S2] while the account of the dipole-dipole magnetic coupling is treated exactly. The Lines model is effective and has been successfully used widely in the research field of f-element single-molecule magnets.[S3]

For each of complexes **1** and **2**, there is only one type of *J*.

The exchange Hamiltonian is:

$$\hat{H}_{exch} = -J_{total}\,\hat{\tilde{S}}_{Dy1}\,\hat{\tilde{S}}_{Dy1a}$$

The J_{total} is the parameter of the total magnetic interaction ($J_{total} = J_{diploar} + J_{exchange}$) between magnetic center ions. The $\hat{\tilde{S}}_{Dy} = \pm 1/2$ are the ground pseudospin on the Dy(III) sites. The dipolar magnetic coupling can be

calculated exactly, while the exchange coupling constants were fitted through comparison of the computed and measured magnetic susceptibility and molar magnetization using the POLY_ANISO program.[S4]

The calculated eight lowest calculated Kramers doublets (KDs) and the ***g*** tensors of complexes **1** and **2** using CASSCF/RASSI are shown in Tables S5.

Table S6. Calculated energy levels (cm^{-1}), ***g*** (g_x, g_y, g_z) tensors and m_J values of the lowest Kramers doublets (KDs) of the Dy fragments of complexes **1** and **2**.

KDs	Complex **1**			Complex **2**		
	E/cm^{-1}	***g***	m_J	E/cm^{-1}	***g***	m_J
1	0.0	0.052 0.117 19.096	±15/2	0.0	0.108 0.215 19.364	±15/2
2	65.6	0.661 1.108 17.433	±3/2	109.7	1.332 4.792 12.734	±11/2
3	99.2	0.859 2.761 13.729	±13/2	145.9	2.556 3.336 11.451	±7/2
4	156.5	8.289 7.990 3.811	±5/2	189.1	8.706 5.493 1.891	±3/2
5	195.0	0.055 2.948 11.692	±7/2	250.2	0.946 1.489 14.289	±1/2
6	239.7	0.948 1.335 15.886	±9/2	316.2	0.295 0.453 18.878	±13/2
7	298.4	0.390 1.101 18.349	±1/2	398.2	0.137 0.261 18.026	±5/2
8	368.6	0.032 0.073 19.651	±11/2	464.0	0.018 0.036 19.198	±9/2

Table S7. Exchange energies (cm^{-1}) and main values of the g_z for the lowest two exchange doublets of **1** and **2**.

	Complex **1**		Complex **2**	
	E	g_z	E	g_z
1	0.0	0.000	0.0	0.000
2	2.4	38.181	2.7	38.718

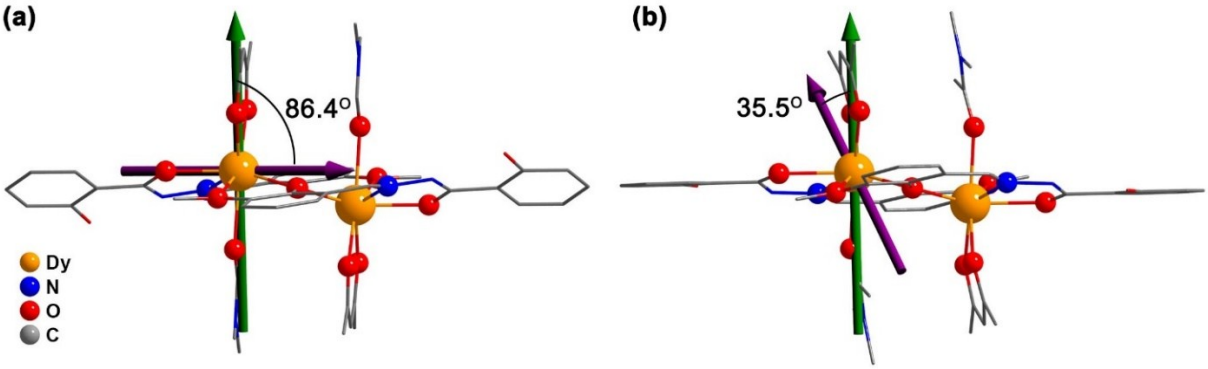

Figure S10. Orientation of the local main magnetic axes of the ground (green arrow) and the first exited (purple arrow) Kramers doublets on one Dy(III) of complexes **1** (a) and **2** (b). Part of the atoms in DBM^- ligands have been omitted for clarity.

Table S8. Natural Bond Order (NBO) charges per atoms in the ground state of complexes **1** and **2** calculated within CASSCF.

	Atoms	**1**	Atoms	**2**
	Dy1	2.547	Dy1	2.544
Atoms of hard plane	O1	−0.790	O1	−0.782
	O1a	−0.797	O1a	−0.797
	O2	−0.454	O2	−0.414
	O3a	−0.783	O3a	−0.670
	N1	−0.279	N1	−0.257
	Average	−0.621	Average	−0.584
Axial coordination atoms	O6	−0.746	O5	−0.768
	O7	−0.768	O6	−0.776
	O5	−0.678	O7	−0.730
	Average	−0.731	Average	−0.758

Reference:

S1 Karlström, G.; Lindh, R.; Malmqvist, P. -Å.; Roos, B. O.; Ryde, U.; Veryazov, V.; Widmark, P. -O.; Cossi, M.; Schimmelpfennig, B.; Neogrady, P.; Seijo, L. MOLCAS: a Program Package for Computational Chemistry. *Comput. Mater. Sci*. **2003**, *28*, 222.

S2 Lines, M. E. *J. Chem. Phys.* **1971**, *55*, 2977.

S3 (a) Mondal, K. C.; Sundt, A.; Lan, Y. H.; Kostakis, G. E.; Waldmann, O.; Ungur, L.; Chibotaru, L. F.; Anson, C. E.; Powell, A. K. *Angew. Chem. Int. Ed*. **2012**, *51*, 7550. (b) Langley, S. K.; Wielechowski, D. P.; Vieru, V.; Chilton, N. F.; Moubaraki, B.; Abrahams, B. F.; Chibotaru, L. F.; Murray, K. S. *Angew. Chem. Int. Ed*. **2013**, *52*, 12014.

S4 (a) Chibotaru, L. F.; Ungur, L.; Soncini, A. *Angew. Chem. Int. Ed*., **2008**, *47*, 4126. (b) Ungur, L.; Van denHeuvel, W.; Chibotaru, L.F. *New J. Chem*., **2009**, *33*, 1224. (c) Chibotaru, L. F.; Ungur, L.; Aronica,C.; Elmoll, H.; Pilet, G.; Luneau, D. *J. Am. Chem. Soc*., **2008**, *130*, 12445.